response, however, decreases steadily with decreasing pH because of loss of the electroactive species. Very similar behavior has been reported for other peptido complexes of nickel.[35] The E_p values for the **4**-L complexes in DMF are very close (±20 mV) to those recorded in aqueous borate buffer (Table IV). Since the **4**-L complexes were generated in situ for the electrochemical measurements, their electronic spectra were checked before and after the experiments to ensure integrity of the electroactive species. The E_p values and the absorption spectra of **4**-Im and **4**-py do not change appreciably with further addition of Im and py, respectively. This shows that axial coordination of L to nickel in **4**-L does not occur under the experimental conditions.[36]

Summary

The following are the principal results and conclusions of this investigation.

(1) A trimeric thiolato-bridged Ni(II) complex (**3**) of *N*-(2-mercaptopropionyl)glycine (**1**) has been isolated and structurally characterized. The complex contains a novel Ni_3S_3 trigonal-antiprismatic core. Among nickel complexes of S-containing peptides, the structure of **3** is the first one to be determined. It has been established that a previously reported complex of the composition $Na[Ni(C_5H_6NO_3S)(H_2O)]$[8c] should be formulated as $Na_3[Ni_3(C_5H_6NO_3S)_3]\cdot 3H_2O$, i.e., the Na^+ salt of **3**.

(2) Addition of L (L = py, Im, CN^-) to solutions of **3** in various protic and aprotic solvents results in bridge-splitting with concomitant generation of the monomeric complexes $[Ni(C_5H_6NO_3S)L]^{n-}$ (n = 1, 2), **4**-L. The structures of the **4**-L complexes have been elucidated by various spectroscopic techniques.

(3) Electrochemical experiments have shown that **3** and **4**-L (L = py, Im, CN^-) are irreversibly oxidized to unstable Ni(III) species in aqueous and DMF solutions. The E_p values for oxidation lie in the range of +0.30 to +0.40 V vs SCE. These values are *lower* than the usual half-wave potentials (+0.55 to +0.72 V vs SCE) observed with the various peptido complexes of nickel.

Acknowledgment. This research was supported by a grant from the Universitywide Energy Research Group of UC and a grant from UCSC "SEED" Funds at the University of California, Santa Cruz. We thank Arman Faroghi for help in the initial synthetic attempts.

Supplementary Material Available: Disposition of the three coordination planes of the three Ni centers in the anion of **3** (Figure S1), electronic absorption spectra of $Na[Ni(C_5H_6NO_3S)(H_2O)]$ and **3** in aqueous borate buffer (Figure S2), variations in the positions of the ^{13}C resonances of MPG in D_2O with increasing pD and of **4**-CN in D_2O (Figure S3), anisotropic thermal parameters for non-hydrogen atoms (Table S1), hydrogen atom parameters (Table S2), short contacts due to hydrogen bonding (Table S3), and atomic coordinates for the atoms of the solvents of crystallization (Table S4) (6 pages); values of $10|F_o|$ and $10|F_c|$ (Table S5) (24 pages). Ordering information is given on any current masthead page.

(35) Bossu, F. P.; Margerum, D. W. *Inorg. Chem.* **1977**, *16*, 1210.
(36) Murry, C. K.; Margerum, D. W. *Inorg. Chem.* **1982**, *21*, 3501.

Contribution from Ames Laboratory,[1] USDOE, and the Department of Chemistry, Iowa State University, Ames, Iowa 50011

Synthesis, Structure, and ^{31}P NMR Spectra of $Mo_2W_2Cl_8(PR_3)_4$ Rectangular Clusters

Richard T. Carlin and Robert E. McCarley*

Received November 2, 1988

The new compounds $Mo_2W_2Cl_8(PMe_3)_4\cdot C_4H_8O$ (I) and $Mo_2W_2Cl_8[P(n\text{-}Bu)_3]_4$ (II) have been prepared by cycloaddition reactions of $MoW(O_2CCMe_3)_4$. Yellow-green crystals of I provided crystallographic data for a complete structure determination: tetragonal, space group $P4_22_12$, a = 12.6443 (8) Å, c = 11.2854 (9) Å, V = 1804.3 Å^3, Z = 2, R = 0.034, R_w = 0.045. Disordering of the Mo and W atoms on the metal atom sites permits only averaged M—M, M—Cl, and M—P distances for the rectangular cluster units. Of principal interest were the M≡M and M—M distances of 2.275 (1) and 2.842 (1) Å, respectively, for the short and long edges of the Mo_2W_2 rectangular cluster units. A study of the $^{31}P\{^1H\}$ NMR spectrum for a solution of II showed that coupling of the Mo–W dinuclear units provided two isomers, IIa and IIb, in a ratio of ca. 1.5:1.0. Isomer IIa was assigned as arising from head-to-tail coupling, and IIb as arising from head-to-head coupling of the two MoW units. Electronic spectral data for II are also reported.

Introduction

The recent synthesis of the quadruply bonded dinuclear complexes $MoWCl_4(PR_3)_4$[2] sparked interest in the possibility for the preparation of the tetranuclear compounds $Mo_2W_2Cl_8(PR_3)_4$. The homonuclear analogues, $Mo_4Cl_8(PR_3)_4$[3-5] and $W_4Cl_8(PR_3)_4$,[4,5] have both been prepared. These homonuclear tetranuclear complexes have a rectangular framework of metal atoms with two unbridged, short sides and two long sides bridged by chlorines or bromines. Each metal has a distorted square-planar coordination. The bond distances in the rectangle suggest that the short, unbridged edges are M–M triple bonds and the long, halide-bridged edges are M–M single bonds.

The formation of these tetranuclear species is unique because it can be viewed as a cycloaddition of two dinuclear units.[3] This cycloaddition involves loss of the δ component of the quadruple bond in each dinuclear unit and formation of two single bonds that join the two units together.[3,6] The reaction is believed to be initiated by loss of phosphine ligand with subsequent formation of the metal–metal single bonds.[3]

Using techniques similar to those used for preparation of the homonuclear analogues,[3,5] it has been possible to synthesize $Mo_2W_2Cl_8(PMe_3)_4$ and $Mo_2W_2Cl_8(PBu_3)_4$. The characterization of these mixed-metal compounds has been accomplished by using ^{31}P NMR spectra, UV–visible spectra, and an X-ray single-crystal study.

Experimental Section

Materials. All reaction products were handled in Schlenk vessels under a nitrogen atmosphere or under vacuum. Tetrahydrofuran and cyclohexane were dried and handled as discussed earlier.[2a] Methanol was dried over sodium methoxide and vacuum-distilled onto molecular sieves (4 Å) for storage. Trimethylphosphine and tri-*n*-butylphosphine were obtained from Alpha Products and Strem Chemicals, respectively, and were used without further purification. Chlorotrimethylsilane was ob-

(1) Ames Laboratory is operated for the US Department of Energy by Iowa State University under Contract No. W-7405-Eng-82. This research was supported by the Office of Basic Energy Sciences.
(2) (a) Carlin, R. T. Ph.D. Dissertation, Iowa State University, Ames, IA, 1982; Section II. (b) Luck, R. L.; Morris, R. H.; Sawyer, J. F. *Inorg. Chem.* **1987**, *26*, 2422.
(3) Ryan, T. R.; McCarley, R. E. *Inorg. Chem.* **1982**, *21*, 2072.
(4) McCarley, R. E.; Ryan, T. R.; Torardi, C. C. *Reactivity of Metal-Metal Bonds*; Chisholm, M. H., Ed.; ACS Symposium Series 155; American Chemical Society: Washington, DC, 1981; p 41.
(5) Ryan, T. R. Ph.D. Dissertation, Iowa State University, Ames, IA, 1981; Sections II and III.
(6) Wheeler, R. A.; Hoffmann, R. *J. Am. Chem. Soc.* **1986**, *108*, 6605.

0020-1669/89/1328-3432$01.50/0

Table I. Crystallographic Data for $Mo_2W_2Cl_8[P(CH_3)_3]_4 \cdot C_4H_8O$

formula $Mo_2W_2Cl_8P_4C_{16}H_{44}O$	fw 1219.62
a = 12.6443 (8) Å	space group $P4_22_12$
c = 11.2854 (9) Å	T = 22 °C
V = 1804.3 (2) Å^3	λ = 0.710 34 Å
Z = 2	ρ_{calcd} = 2.245 g cm^{-3}
$R(F_o)$ = 0.034	μ = 81.4 cm^{-1}
$R_w(F_o)$ = 0.045	

tained from Fisher Scientific Co. and was used without further purification. Aluminum trichloride obtained from Fisher Scientific Co. was purified by sublimation.

Physical Measurements. Electronic spectra were obtained by using a Cary 14 spectrophotometer. Samples for ^{31}P NMR study were dissolved in $CDCl_3$ and sealed in vacuo in 10-mm NMR tubes along with a capillary containing a H_3PO_4 standard. The ^{31}P NMR spectra were obtained by using a Bruker WM-300 spectrometer (121.4 MHz). X-ray powder diffraction data were obtained by using an Enraf-Nonius Delft triple-focusing Guinier X-ray powder diffraction camera with Cu $K\alpha_1$ radiation (λ = 1.540 56 Å).

$MoW(O_2CCMe_3)_4$. This extremely air-sensitive compound was prepared in limited quantities by a multistep procedure devised by Katovic et al.[7]

$Mo_2W_2Cl_8(PMe_3)_4$. With use of a N_2 drybox, $MoW(O_2CCMe_3)_4$ (0.22 g, 0.32 mmol) and $AlCl_3$ (0.2 g, 1.5 mmol) were introduced into a 100-mL reaction flask. Trimethylphosphine (0.06 mL, 0.6 mmol) and 30 mL of THF were then vacuum-distilled into the flask. The reaction mixture was stirred at reflux for 1 day. Upon filtration, a blue-green filtrate (indicating formation of a significant amount of $MoWCl_4(PMe_3)_4$) and a small quantity of a yellow-green solid were obtained. This yellow-green solid was extracted with the mother liquor under reduced pressure. The mother liquor was refiltered, giving insoluble yellow-green crystals that were suitable for X-ray single-crystal analysis.

$Mo_2W_2Cl_8[P(n\text{-}Bu)_3]_4$. $MoW(O_2CCMe_3)_4$ (0.5 g, 0.73 mmol), $AlCl_3$ (0.39 g, 2.9 mmol), and PBu_3 (0.35 mL, 1.4 mmol) were refluxed under nitrogen in 20 mL of THF for ca. 1 day. The dark green solution was filtered; however, no solid was obtained. The solvent was removed in vacuo, giving a green tar to which was added 15 mL of methanol. Filtering of the methanol solution gave a dark green filtrate and a yellow-green solid. The methanol solution was discarded. The yellow-green solid was dried in vacuo and then extracted with cyclohexane to obtain crystals. Indexing two of these crystals confirmed them to be isomorphous with the corresponding $P(n\text{-}Bu)_3$ derivatives of the molybdenum[8] and tungsten[5] homonuclear analogues.[9] The crystals, however, exhibited weak diffracting characteristics, and so no single-crystal X-ray data were collected.

$Mo_4Cl_8(PMe_3)_4$. $Mo_2(OCCH_3)_4$ (1.0 g, 2.3 mmol), $AlCl_3$ (1.25 g, 9.4 mmol), and PMe_3 (5.2 mmol obtained by heating 1.13 g of AgI·PMe_3) were stirred under nitrogen in 30 mL of THF for 18 h. The reaction mixture was filtered, and the resulting light green solid was washed with deoxygenated methanol and dried in vacuo. Comparison of the X-ray powder patterns of this product and those of the mixed-metal PMe_3 derivative confirmed them to be isomorphous.

Collection and Treatment of X-ray Data

The crystal selected was irregularly shaped with dimensions 0.2 × 0.14 × 0.2 mm. It was mounted in a 0.3-mm glass capillary, and this setup was placed on a four-circle diffractometer designed at the Ames Laboratory.[10] All crystallographic procedures and calculations were performed as previously described.[11] Important crystallographic data are listed in Table I.

Structure Solution and Refinement

Systematic extinctions for $h00$ ($h = 2n + 1$), $0K0$ ($k = 2n + 1$), and $00l$ ($l = 2n + 1$) uniquely determined the space group as the acentric group $P4_22_12$. All refinements were carried out by using either block-matrix or full-matrix least-squares procedures minimizing the function $\sum w(|F_o| - |F_c|)^2$, where $w = 1/\sigma F_2$. Scattering factors for all non-metals were obtained from Hanson et al.[12]

A sharpened Patterson map revealed the position of the one independent metal atom. This metal atom was input by using a scattering factor table calculated by averaging the molybdenum and tungsten tables. The real and imaginary parts of anomalous dispersion were calculated also by averaging together the appropriate molybdenum and tungsten tables.[13] By use of a combination of least-squares refinements and Fourier synthesis techniques, all non-hydrogen atoms were located and refined to residuals of R = 0.045 and R_w = 0.078. Idealized hydrogen positions were calculated by setting d(C–H) = 0.95 Å and H–C–H = 109.47°. These positional parameters as well as the isotropic B values of 7.0 Å^2 were held constant throughout the remainder of the refinement. Including these fixed hydrogens in the refinement gave lower residuals of R = 0.040 and R_w = 0.047 and lowered the residuals of the low-angle data by ca. 1 to 2%.

At this point, another difference Fourier synthesis revealed the presence of a diffuse and highly disordered THF molecule. Summation over the positive residual electron density showed there to be ca. one THF molecule per tetranuclear unit. By use of three carbon atoms (C1s, C2s, and C3s) in general positions, a reasonable fit to the THF electron density was obtained. Inclusion of this THF molecule in the refinement gave R = 0.035 and R_w = 0.045 and dramatically improved the low-angle data (sin θ < 0.2) by several percent.

A secondary extinction factor of 0.000 20 (5) was obtained, and final residuals of R = 0.034 and R_w = 0.045 resulted after full-matrix least-

Table II. Positional Parameters for $Mo_2W_2Cl_8(PMe_3)_4 \cdot THF$ Non-Hydrogen Atoms[a]

atom	x	y	z
MoW[b]	0.08243 (5)	0.07636 (5)	0.10069 (5)
Clt	0.1092 (3)	0.2489 (3)	0.1922 (3)
Clb	−0.1037 (3)	0.1084 (3)	0.1453 (3)
P	0.2806 (3)	0.0669 (3)	0.1243 (3)
C1	0.361 (1)	0.181 (1)	0.085 (1)
C2	0.349 (1)	−0.043 (1)	0.051 (2)
C3	0.314 (2)	0.047 (2)	0.284 (2)
C1s	0.434 (3)	0.504 (4)	0.081 (3)
C2s	0.530 (6)	0.412 (5)	0.009 (9)
C3s	0.545 (5)	0.583 (5)	0.035 (6)

[a] Estimated standard deviations are given in parentheses for the last significant figures. [b] The symbol MoW means that either Mo or W may be present.

Table III. Bond Distances (Å) and Angles (deg) for the $Mo_2W_2Cl_8(PMe_3)_4$ Molecule[a]

	Distances		
MoW–MoW[b]	2.275 (1)	MoW–P	2.523 (4)
MoW–MoW	2.842 (1)	P–C1	1.82 (1)
MoW–Clt	2.437 (4)	P–C2	1.83 (2)
MoW–Clb	2.405 (4)	P–C3	1.86 (2)
MoW–Clb	2.440 (4)		
	Angles		
MoW–MoW–MoW	89.90 (0)	Clb–MoW–Clb	103.0 (1)
MoW–MoW–Clt	135.2 (1)[c]	Clt–MoW–P	81.9 (1)
MoW–MoW–Clt	113.45 (9)	Clb–MoW–P	79.7 (1)
MoW–MoW–Clb	53.52 (9)[c]	Clb–MoW–P	160.7 (1)
MoW–MoW–Clb	54.67 (9)[c]	MoW–Clb–MoW	71.8 (1)
MoW–MoW–Clb	99.66 (8)	MoW–P–C1	119.3 (5)
MoW–MoW–Clb	99.66 (8)	MoW–P–C2	117.0 (5)
MoW–MoW–Clb	104.21 (8)	MoW–P–C3	109.5 (6)
MoW–MoW–P	98.09 (9)	C1–P–C2	103.4 (7)
MoW–MoW–P	134.1 (1)[c]	C1–P–C3	102.2 (8)
Clt–MoW–Clb	84.1 (1)	C2–P–C3	103.2 (9)
Clt–MoW–Clb	139.9 (1)		

[a] Estimated standard deviations are given in parentheses for the last significant figures. [b] The symbol MoW indicates that either Mo or W could be present. [c] Angles for which the MoW–MoW vector is the long MoW–MoW separation in the tetramer.

(7) Katovic, V.; Templeton, J. L.; Hoxmeier, R. J.; McCarley, R. E. *J. Am. Chem. Soc.* **1975**, *97*, 5300.
(8) Lii, K. H.; McCarley, R. E. Iowa State University, Ames, IA, unpublished results.
(9) Average lattice parameters obtained from indexing two crystals of $Mo_2W_2Cl_4(PBu_3)_4$: a = 27.45 Å, b = 37.00 Å, c = 14.60 Å, α = 89.15°, β = 88.8°, γ = 91.4°. The homonuclear tetramers' unit cells are orthorhombic ($\alpha = \beta = \gamma = 90°$) with the following dimensions: $Mo_4Cl_8(PBu_3)_4$, a = 26.654 (3) Å, b = 36.403 (3) Å, c = 14.437 (3) Å;[7] $W_4Cl_8(PBu_3)_4$, a = 26.990 (9) Å, b = 36.302 (9) Å, c = 14.293 (6) Å.[5]
(10) Rohrbaugh, W. J.; Jacobson, R. A. *Inorg. Chem.* **1974**, *13*, 2535.
(11) Lii, K.-H.; McCarley, R. E.; Kim, S.; Jacobson, R. A. *J. Solid State Chem.* **1986**, *64*, 347.
(12) Hanson, H. P.; Herman, F.; Lea, J. D.; Skillman, S. *Acta Crystallogr.* **1960**, *17*, 1040.
(13) Templeton, D. H. In *International Tables for X-ray Crystallography*, 1st ed.; Macgillary, C. H., Rieck, G. D., Eds.; Kynoch Press: Birmingham, England, 1962; Vol. III, p 215.

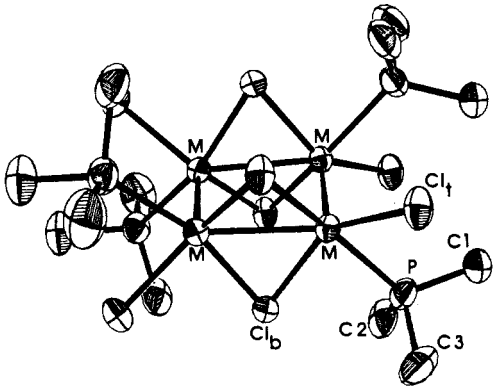

Figure 1. Structure of the $Mo_2W_2Cl_8(PMe_3)_4$ molecule (50% probability thermal ellipsoids). Disordered Mo and W positions shown as M.

Table IV. Bond Distances (Å) and Angles (deg)[a] in Rectangular Cluster Compounds

	$Mo_2W_2Cl_8(PMe_3)_4$	$Mo_4Cl_8[P(n\text{-}Bu)_3]_4$[b]	$W_4Cl_8[P(n\text{-}Bu)_3]_4$[c]
$M-M_{short}$	2.275 (1)	2.214 (4)	2.309 (2)
$M-M_{long}$	2.842 (1)	2.904 (3)	2.840 (1)
M–Clt	2.437 (4)	2.406 (6)	2.400 (5)
M–Clb (cis P)	2.405 (4)	2.406 (6)	2.396 (5)
M–Clb (trans P)	2.440 (4)	2.417 (6)	2.417 (5)
M–P	2.523 (4)	2.551 (4)	2.530 (5)
M–M–M	89.90 (0)	89.94 (1)	89.93 (3)
M–Clb–M	71.8 (1)	74.0 (2)	72.3 (1)
Clb–M–Clb	103.0 (1)	100.5 (2)	102.8 (2)

[a] Estimated standard deviations are given in parentheses for the last significant figures. [b] Reference 8. [c] Reference 5.

squares refinement. The final difference Fourier synthesis was clean with the largest peak of 0.8 e/Å^3 found between intracluster metal atoms. Peaks of ca. 0.5 e/Å^3 were seen in the region of the THF molecule. Final positional parameters are given in Table II, and bond distances and angles are listed in Table III.

Results and Discussion

Crystal Structure. The basic structure of the mixed-metal tetranuclear species, shown in Figure 1, is essentially that expected from examination of the homonuclear analogues.[3-5] The metal atoms form a rectangle with two long M–M bonds, 2.842 (1) Å, and two short M–M bonds, 2.275 (1) Å. As has been discussed for the homonuclear cases, the heteronuclear rectangle can be viewed as being formed by the cycloaddition of two quadruply bonded units of formulation $MoWCl_4(PR_3)_4$.[2] The long M–M bond is formed by σ overlaps of the d_{xy} orbitals on the metal atoms with subsequent loss of the δ interactions in the dinuclear units, reducing the quadruple bonds to formal triple bonds. In Table IV are listed the important parameters for comparison of the heteronuclear compound to the homonuclear analogues.[5,8] The homonuclear complexes containing $P(n\text{-}Bu)_3$ ligands were chosen because the ligand arrangement about these complexes is of D_2 symmetry, the same as in the mixed-metal compound.

An examination of the M–L bond lengths for the series of compounds in Table IV reveals three apparent anomalies in the mixed-metal tetranuclear molecule: (1) a short M–P bond, (2) a long M–Clt bond, and (3) a long M–Clb bond. The M–P bond of 2.520 (4) Å is actually equal to the average M–P bond length in $MoWCl_4(PMe_3)_4$.[2] The M–P distance is that expected when compared to the M–P distances found in the molybdenum and tungsten dinuclear analogues.[2] Apparently, $M-PMe_3$ bonds are 0.1–0.2 Å shorter than $M-P(n\text{-}Bu)_3$ bonds in these compounds; therefore, the shortness of the M–P bond in the heteronuclear case is due to the bonding characteristics of PMe_3 and not to the metals present.

Because the $M-PMe_3$ bond is considerably shorter than the $M-P(n\text{-}Bu)_3$ bonds, PMe_3 should have a greater trans influence than $P(n\text{-}Bu)_3$. This is most likely the reason for the unusually long M–Clb bond in the mixed-metal compound, since it is this bond that is trans to PMe_3. This same trans influence is seen in the homonuclear analogues, but to a lesser degree. The other M–Clb bond, trans to Clt, in the mixed-metal compound is an average of the corresponding M–Clb bond lengths found in the Mo and W homonuclear complexes.

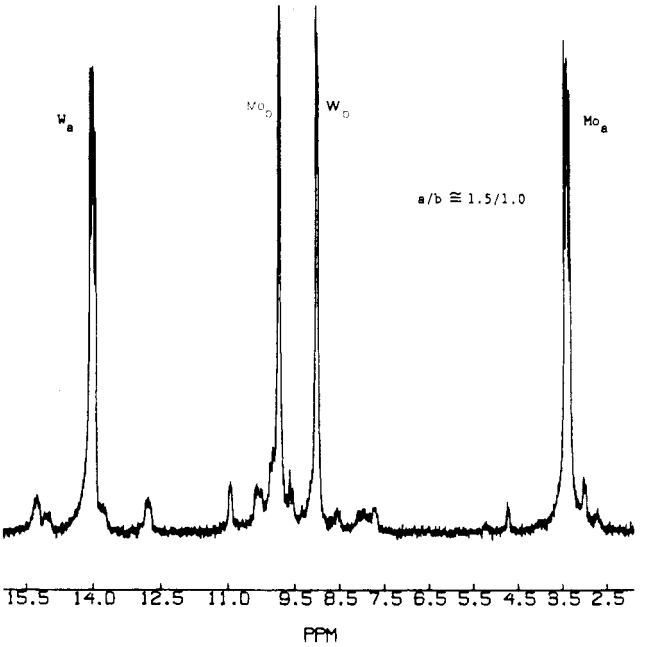

Figure 2. $^{31}P\{^1H\}$ NMR spectrum (121.4 MHz) of $Mo_2W_2Cl_8[P(n\text{-}Bu)_3]_4$ in $CDCl_3$ solution.

There is no apparent reason for the unusually long M–Clt distance in the mixed-metal compound, except that it too may be a result of bonding properties of PMe_3.

A discussion of the metal–metal bond distances in the heteronuclear compound based solely on its crystal structure would be ambiguous because of the inability to distinguish between Mo and W atoms in the structure. Although the M–M triple bonds on the short edges will both be Mo–W bonds, isomers may exist where the two single bonds could be either two Mo–W bonds or one Mo–Mo bond and one W–W bond. The ^{31}P NMR results discussed next distinguish between these two metal isomers.

^{31}P NMR Spectra. Because of the low solubility of $Mo_2W_2Cl_8(PMe_3)_4$ in all common organic solvents, it was impossible to obtain a ^{31}P NMR spectrum of this derivative. For the tri-*n*-butylphosphine heteronuclear complex, however, solubility in $CDCl_3$ was sufficient to obtain a spectrum. The full proton-decoupled ^{31}P NMR spectrum of $Mo_2W_2Cl_8[P(n\text{-}Bu)_3]_4$, shown in Figure 2, consists of a set of intense doublets centered at 9.04 and 9.88 ppm and two intense multiplets centered at 3.48 and 14.02 ppm. The two multiplets correspond to one isomer, isomer a, and the two doublets result from the presence of another isomer, isomer b. The relative concentration of isomer a to isomer b is ca. 1.5:1.0. Small peaks in Figure 2 arise from isotopomers containing one ^{183}W nucleus (24% of total ^{31}P intensity). Assignment of these resonances requires examination of both the P–P and W–P couplings.

The intense multiplets for isomer a are in fact doublets of doublets with P–P coupling constants of 8.5 and 5.9 Hz. This is apparent from Figure 3, which shows a magnified view of the multiplet centered at 14.02 ppm. To obtain such a coupling scheme, it is necessary to have an isomeric arrangement of metal atoms in which Mo and W alternate around the tetramer as shown in the Figure 3 insert. In this isomer, an AA'XX' system when ^{183}W coupling is ignored, each phosphorus atom on tungsten is coupled to two equivalent phosphorus atoms bound to molybdenum. Because the two molybdenums are bonded differently to tungsten, the coupling constants of each phosphorus atom on tungsten to the phosphorus atoms on the two molybdenums will be different, thus giving rise to the observed doublet of doublets. The same coupling scheme is seen for the phosphorus atoms bound

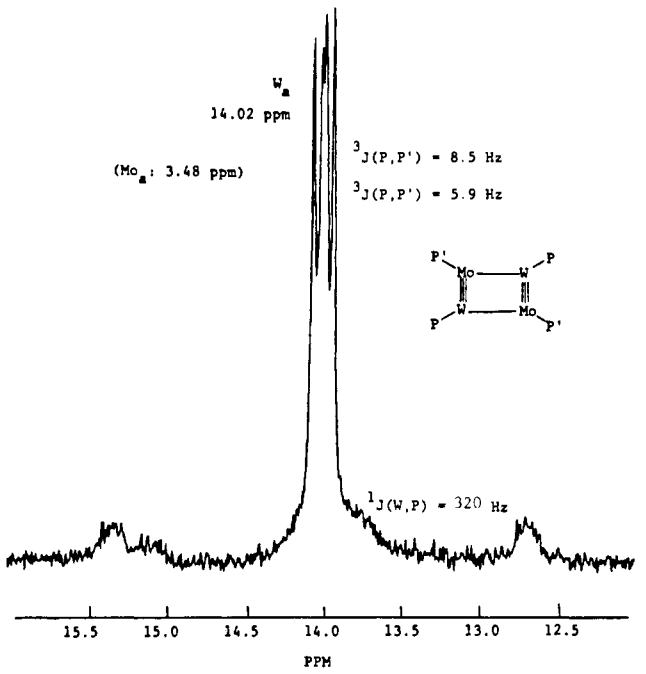

Figure 3. Expanded view of multiplet centered at 14.02 ppm in $^{31}P\{^1H\}$ NMR spectrum (121.4 MHz) of $Mo_2W_2Cl_8[P(n\text{-}Bu)_3]_4$. Isomer a giving rise to this resonance is shown in the figure. The other resonance for isomer a is at 3.48 ppm.

to molybdenum. Unambiguous assignment of the two coupling constants to coupling across the single or triple bond is not possible. Coupling across a heteronuclear quadruple bond has been found to be 24.7 Hz in $MoWCl_4(PMe_3)_4$.[2] The two coupling constants observed in this tetranuclear isomer have similar values. It would seem most likely that the larger of the two coupling constants should be assigned to the coupling across the triple bond. This assignment can only be made tentatively, since the presence of the bridging chlorine atoms across the single bond may increase the coupling process across this longer bond.

Figure 4 shows a magnified view of the resonances assigned to isomer b. Again, when coupling to ^{183}W is initially ignored, the single P–P coupling constant of 3.2 Hz observed for the two doublets can be explained by an isomeric arrangement of metal atoms in which the long bonds of the rectangle consist of one Mo–Mo bond and one W–W bond. With this arrangement, the two phosphorus atoms on the tungsten atoms are equivalent and thus no coupling across the long bond is observed; however, these phosphorus atoms are coupled across the triple bond to one of the two equivalent phosphorus atoms on molybdenum.

Assignment of resonances to phosphorus atoms bound to tungsten or to molybdenum can be made by looking for the presence of W–P coupling. Now it becomes necessary to consider isomer a as an AA′MM′X system, where A and M are chemical shift nonequivalent ^{31}P nuclei and X is a ^{183}W nucleus. For isomer a, the resonance at 14.02 ppm is unambiguously assigned to phosphorus bound to tungsten, since resonances resulting from $^1J_{PW}$ are observed at ca. 160 Hz on both sides of the main resonance, giving $^1J_{PW}$ = 320 Hz. (Although a sharp resonance is seen on the downfield side of the resonance at 3.48 ppm, it must be an impurity, because no corresponding resonance is found on the upfield side.) This value is in accord with other one-bond W–P coupling constants.[14] Longer range W–P coupling, $^2J_{PW}$, may be expected for the phosphorus atoms on Mo; however, no clear low-intensity resonances symmetrically disposed about the main resonance at 3.48 ppm could be identified. Unlike that of isomer b discussed below, the spectrum for isomer a appears as a simple A_2M_2X system.

(14) Pregosin, S.; Kunz, R. W. *^{31}P and ^{13}C NMR of Transition Metal Phosphine Complexes*; Diehl, P.; Fluck, E., Kosfeld, R., Eds.; Springer-Verlag: New York, 1979.

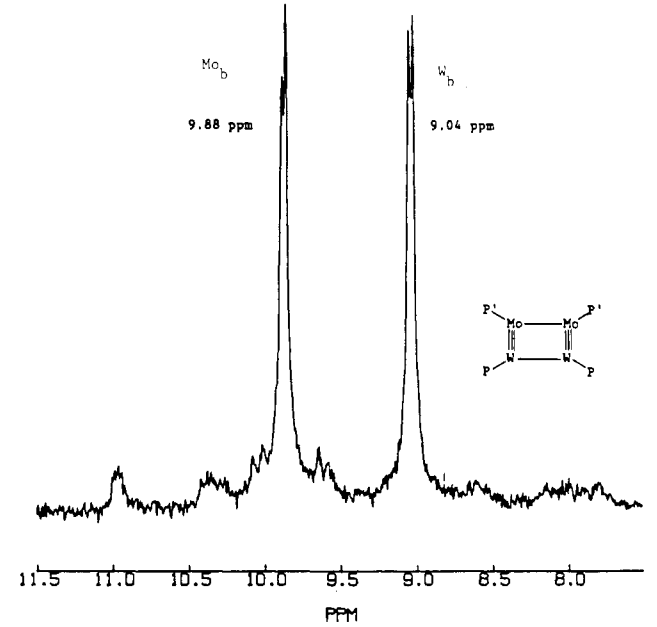

Figure 4. Magnified view of $^{31}P\{^1H\}$ resonances (121.4 MHz) resulting from isomer b (shown in figure) of $Mo_2W_2Cl_8[P(n\text{-}Bu)_3]_4$.

The W–P coupling scheme for isomer b is not as straightforward. Fortunately, a reviewer has graciously simulated the low-intensity resonances observed in Figure 4 based on an AA′MM′X system. The simulation indicates that the major resonance at 9.04 ppm corresponds to phosphorus bound to tungsten and the major resonance at 9.88 ppm is for phosphorus bound to molybdenum. The coupling values determined from the simulation are $J_{AA'} \sim 10$ Hz, $J_{AM} = 3.2$ Hz, $J_{AM'} = 0$ Hz, $J_{AX} = {}^1J_{PW} = 317$ Hz, $J_{A'M} = 0$ Hz, $J_{A'M'} = 3.2$ Hz, $J_{A'X} = {}^2J_{PW} = 20$ Hz, $J_{MM'} = 10$ Hz, $J_{MX} = {}^2J_{PW} = 60$ Hz, and $J_{M'X} = 0$ Hz, where A and M are ^{31}P nuclei on tungsten and molybdenum, respectively, with A bound directly to the ^{183}W nucleus, X. We agree with the assignments provided by the reviewer; however, due to the poor quality of the low-intensity portion of the spectrum, the values of the coupling constants determined in simulation should be regarded as approximate.

The formation of two metal tetranuclear isomers is not totally unexpected. From statistical considerations alone, an exact 50:50 mixture of the two isomers is predicted. Apparently, there is some driving force, either kinetic or thermodynamic, that produces a larger fraction of isomer a over isomer b.

Electronic Spectra. The relevant electronic spectra are shown in Figures 5 and 6. Since the concentrations of most of the solutions used in obtaining the spectra were not determined, the plotted absorption intensities of the curves in each figure are not representative of their relative extinction coefficients. Valuable information can be drawn from comparison of the relative curve shapes and the position of absorption maxima.

Figure 5 shows the electronic spectra of the three $P(n\text{-}Bu)_3$ derivatives.[5] It is immediately apparent that the spectra of the heteronuclear and of the tungsten homonuclear complexes are almost identical at wavelengths below 350 nm. They each exhibit a large maximum at ca. 297 nm with a shoulder on the low-energy side. The UV–visible spectrum of the tetramolybdenum species shows a maximum at 312 nm with no low-energy shoulder. At wavelengths above 350 nm, the spectrum of the heteronuclear cluster appears to be an average of the spectra of the homonuclear clusters.

In Figure 6 plots of both the PMe_3 and $P(n\text{-}Bu)_3$ heteronuclear clusters' spectra are shown together. They are essentially identical, exhibiting maxima at 296 and 297 nm, respectively.

Conclusions

We have shown that the heterodinuclear quadruply bonded complexes $MoWCl_4(PR_3)_4$[2] can be condensed to form the heteronuclear rectangular clusters $Mo_2W_2Cl_8(PR_3)_4$ in the same way

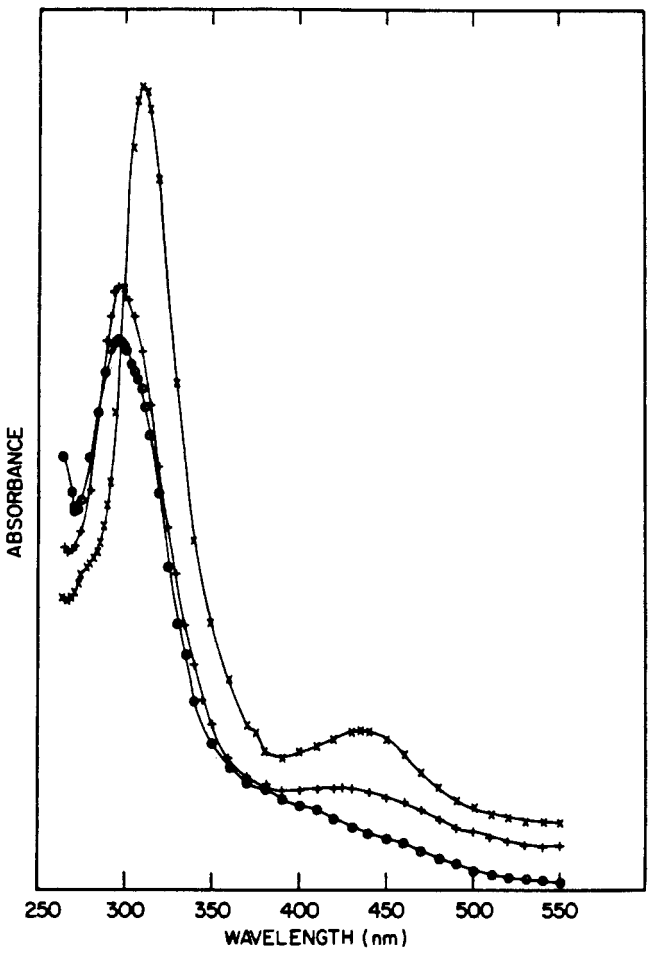

Figure 5. Electronic spectra of $Mo_4Cl_8[P(n\text{-}Bu)_3]_4$ (×), $Mo_2W_2Cl_8[P(n\text{-}Bu)_3]_4$ (+), and $W_4Cl_8[P(n\text{-}Bu)_3]_4$ (o).

that the homonuclear species $M_4Cl_8(PR_3)_4$ (M = Mo or W) can be obtained.[3-5] The studies of $^{31}P\{^1H\}$ NMR spectra show that both head-to-tail (isomer a) and head-to-head (isomer b) coupling of the Mo≡W units occurs when the Mo_2W_2 cluster is formed. Formation of the third isomer of $Mo_2W_2Cl_8(PR_3)_4$ having Mo≡Mo and W≡W bonds on the short edges of the rectangle would require coupling of $Mo_2Cl_8(PR_3)_4$ to $W_2Cl_8(PR_3)_4$, and is not observed.

The geometric disposition of the PMe_3 ligands in $Mo_2W_2Cl_8(PMe_3)_4$ gives rise to the isomer having D_2 symmetry, as also observed for $Mo_4Cl_8[P(n\text{-}Bu)_3]_4$ and $W_4Cl_8[P(n\text{-}Bu)_3]_4$,[4] but not for $Mo_4Cl_8(PEt_3)_4$, which assumes an arrangement with C_{2h} symmetry.[5] Insufficient data are available to discern the factors determining which of these ligand arrangements should be favored for a particular ligand.

The M—M bonding within the Mo_2W_2 cluster is closer to that of $W_4Cl_8[P(n\text{-}Bu)_3]_4$ than that of $Mo_4Cl_8[P(n\text{-}Bu)_3]_4$. Both the Mo≡W and Mo(W)–Mo(W) distances of the rectangle are closer to the W≡W and W—W distances reported for the W_4 rectangle.[4] Since the Mo≡W bond of $MoWCl_4(PMe_3)_4$[2b] is longer by 0.09 Å than the Mo≡Mo bond of $Mo_2Cl_4(PMe_3)_4$,[15] but only 0.04 Å shorter than the W≡W bond of $W_2Cl_4(PMe_3)_4$,[16] this relationship is perhaps understandable. The longer Mo≡W bond indicates weaker δ–δ bonding in the dimer, which in turn promotes greater availability of these δ orbitals for forming the more stable σ bonds on the long edges of the rectangle,[4] comparable to those in the rectangle of $W_4Cl_8[P(n\text{-}Bu)_3]_4$.

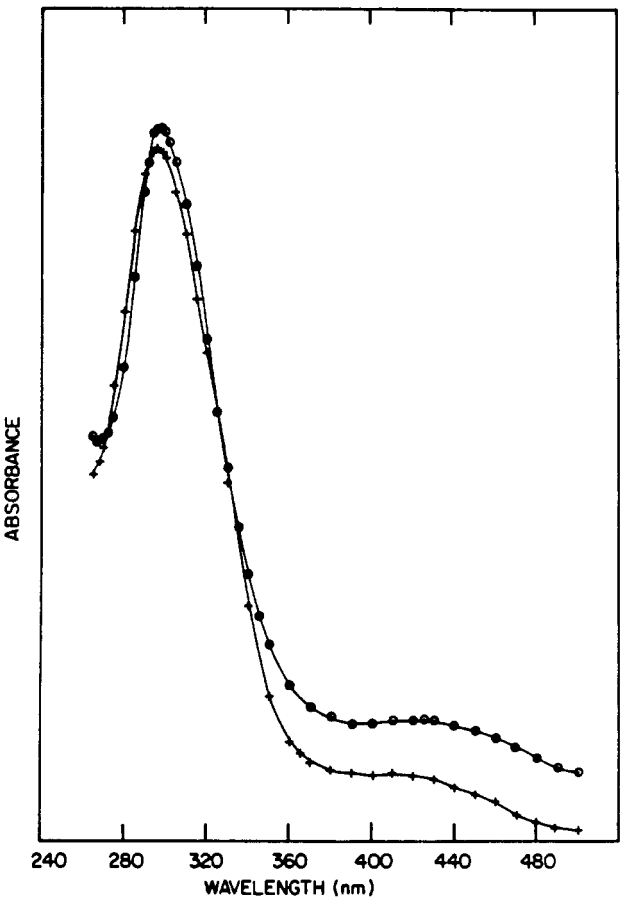

Figure 6. Comparison of the electronic spectra of $Mo_2W_2(PMe_3)_4$ (+) and $Mo_2W_2[P(n\text{-}Bu)_3]_4$ (o).

Acknowledgment. We are grateful to Professor Robert Morris, University of Toronto, who provided the simulation of the ^{31}P NMR spectrum of isomer b discussed above.

Supplementary Material Available: Crystallographic data (Table IS), anisotropic temperature factors (Table IIS), calculated positional parameters for hydrogen atoms (Table IIIS), and a view of the unit cell (Figure IS) (4 pages); observed and calculated structure factors (Table IVS) (3 pages). Ordering information is given on any current masthead page.

(15) Cotton, F. A.; Extine, M. W.; Felthouse, T. R.; Kolthammer, B. W. S.; Lay, D. G. *J. Am. Chem. Soc.* **1981**, *103*, 4040.
(16) Cotton, F. A.; Felthouse, T. R.; Lay, D. G. *J. Am. Chem. Soc.* **1980**, *102*, 1431.